THE ROYAL SOCIETY

*Published online* 28 February 2002

# Spinning an elastic ribbon of spider silk

**David P. Knight**[1*] **and Fritz Vollrath**[1,2]

[1]*Department of Zoology, University of Oxford, South Parks Road, Oxford OX1 3PS, UK*
[2]*Department of Zoology, Universitetsparken B135, 8000 Aarhus C, Denmark*

The Sicarid spider *Loxosceles laeta* spins broad but very thin ribbons of elastic silk that it uses to form a retreat and to capture prey. A structural investigation into this spider's silk and spinning apparatus shows that these ribbons are spun from a gland homologous to the major ampullate gland of orb web spiders. The *Loxosceles* gland is constructed from the same basic parts (separate transverse zones in the gland, a duct and spigot) as other spider silk glands but construction details are highly specialized. These differences are thought to relate to different ways of spinning silk in the two groups of spiders. *Loxosceles* uses conventional die extrusion, feeding a liquid dope (spinning solution) to the slit-like die to form a flat ribbon, while orb web spiders use an extrusion process in which the silk dope is processed in an elongated duct to produce a cylindrical thread. This is achieved by the combination of an initial internal draw down, well inside the duct, and a final draw down, after the silk has left the spigot. The spinning mechanism in *Loxosceles* may be more ancestral.

**Keywords:** extrusion; ultrastructure; elastomer; electron microscopy; brown recluse; *Loxosceles*

## 1. INTRODUCTION

Spider silks show a remarkable range of mechanical properties (Madsen *et al.* 1999; Vollrath *et al.* 2001) with dragline silks in some species of orb web spider exhibiting elastomeric properties when wet and quite exceptional toughness when either wet or dry (Vollrath & Edmonds 1989; Gosline *et al.* 1986). The wide range of mechanical behaviour results from a design adapted over an evolutionary time-span of *ca.* 400 Myr (Shear *et al.* 1989) in both the spinning solution (protein dope) and the spinning conditions (Vollrath & Knight 2001). Recent studies are beginning to use sequence information of the spidroin dopes to reconstruct phylogenetic trees of silk sequence evolution (e.g. Gatesy *et al.* 2001). We have now begun a comparative study of silk gland evolution, and if all goes well then the two trees should overlap, although both sides are still a long way away from this. For such a comparative study of spinneret evolution the spider *Loxosceles* sp. is of particular interest because first, it is not closely related (Hormiga *et al.* 2000; Griswold *et al.* 1998) to the orb weaving spiders which are most often studied for their silk and glands. Second, its major silk is an extremely thin ribbon (Stern & Kullmann 1975). The extrusion of a broad ribbon instead of a cylindrical thread suggested that the mechanism of formation must be different from that used to form the dragline threads in orb web spiders. *Loxosceles* silk, moreover, is rather 'sticky' and closely 'hugs' any objects it touches (Gardner 1998; M.G. Ramirez, personal communication) as in the comparably thin, but round hackled threads of the cribellate spiders (Opell 1995), possibly through electrostatic or van der Waals forces. The brown recluse uses its silk to form a small mat of tangled threads which it extends from a retreat under stones, scraps of wood, dead cactus and similar dry sites (Smith 1982). Currently, neither the structure of the silk gland or of the duct has been described in detail for *Loxosceles*, although Kovoor (1987) mentioned the existence of a large pair of tubular silk glands, assigning them to the ampullate type on account of their shape. Here we describe the structure of the silk ribbons. We discuss the form and function of the spinneret and report that the size and shape of the principal silk gland and the location of its spigot strongly suggest homology with the MA gland of orb web spiders. Furthermore, we describe the highly specific structure of the gland cells in the two transverse zones making up the secretory part of the gland. Finally, we discuss the evolutionary significance of the similarities and differences in construction of the glands in *Loxosceles* and orb web spiders.

## 2. MATERIAL AND METHODS

Brown recluse (fiddle back) spiders, *Loxosceles laeta*, of the family Sicaridae (Araneomorphae) are found mainly in the American mid-west (Smith 1982). We obtained adult female spiders bred in captivity. In the laboratory the spiders readily spin retreats in the holding containers. To mount silk for SEM, stubs covered with double-sided adhesive tape were pushed up through a sheet of silk forming the retreat. These were air-dried and sputter-coated with gold before viewing at 15 kV and a magnification of up to ×12 000. A similar technique was used to mount silk ribbons on lightly carboned formvar-coated grids for TEM. Grids were stained, at 20 °C, with freshly prepared saturated uranyl acetate in 70% v/v ethanol (20 min) and undiluted Reynold's lead citrate (12 min). They were lightly annealed in a widely spread beam and then imaged at 80 kV using low dose technique and magnifications of up to ×40 000.

On arrival in the laboratory, spiders were immediately dis-

*Author for correspondence (knight@tegdown.u-net.com).

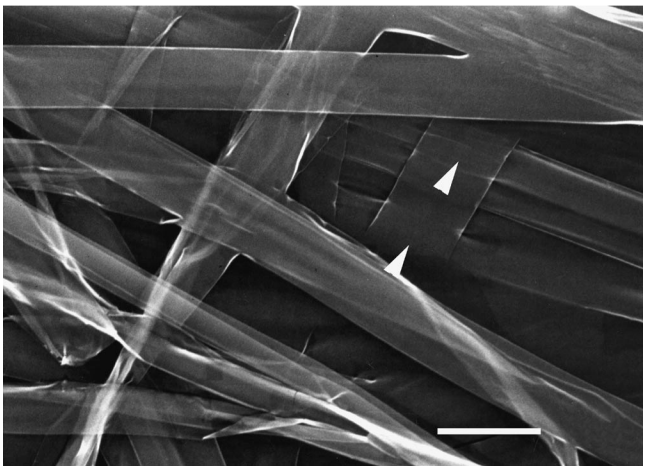

Figure 1. SEM micrograph showing the MA silk from a final-instar female *L. laeta* spider. Plaques of adhesion between ribbons (arrowheads; see text). Scale bar, 10 μm.

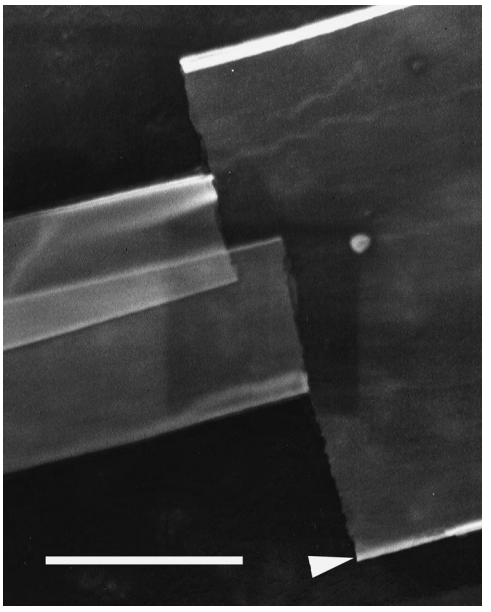

Figure 2. As figure 1 but illustrating a partial fracture of the ribbon (see text). The ribbon is thickened at its edge (arrow). Scale bar, 5 μm.

sected and fixed. The abdominal cavity was promptly irrigated with a Karnovsky fixative containing a final concentration of 2% glutaraldehyde, 2% formaldehyde, 0.1 M of sodium cacodylate, 0.35 M of sodium chloride and 0.01% calcium chloride finally adjusted to pH 7.4 with hydrochloric acid. Fixation was continued for 30 min after which the MA glands were dissected out and fixation continued for 1 h at 4 °C. After washing in buffer, material was post-fixed in buffered 1% osmium tetroxide, dehydrated in alcohols, *en bloc* stained with uranyl acetate and embedded in Spurr's resin using an extended embedding schedule. Ultrathin sections were cut with glass or diamond knives and were examined at 80 kV after staining with alcoholic uranyl acetate and lead citrate, as described above. For SEM, tissue was fixed in the same way and examined after critical point drying and sputtering with gold. For differential interference microscopy, material fixed in the Karnovsky fixative as described above was mounted in Farrant's gum without post-fixation in osmic acid.

## 3. RESULTS AND DISCUSSION

### (a) *Structure of the retreat and silk ribbons*

The spider *L. laeta* spins a retreat underneath objects. These retreats usually consist of two sheets of silk threads with a space between them for the spider and a tangle of looser threads outside the sheets. The lower sheet is in contact with the substratum while the upper sheet, attached to the underside of objects, has a small exit hole (5–10 mm in diameter) for the spider. The sheets are composed of a meshwork of silk ribbons (see below) anchored to surfaces by attachment plaques formed from numerous very fine threads probably derived, as in orb web spiders (Vollrath 1992), from the pyriform glands. Similar plaques are evidently also used to stick new ribbons to the surface of an existing sheet. Probing the meshwork with two pairs of watchmaker's forceps showed that the fine silk ribbons often adhered tightly to one another where they crossed and that the whole network was markedly elastic with individual ribbons capable of stretching up to twice their resting length and returning to it quite rapidly when released. Individual fibres were too short to mount on our mechanical testing instrument.

When viewed using SEM, the silk sheet consisted of broad but extremely thin ribbons (figure 1) with occasional patches of very narrow cylindrical filaments (not shown). Each straight length of ribbon had a remarkably constant width. The mean width of the ribbons was $7.0 \pm 0.7$ μm ($n = 20$), some of the variation probably resulting from the variable extension produced by mounting on SEM stubs. The two edges of the ribbons scattered more electrons than their middles (figure 1) suggesting that a narrow strip along both edges was appreciably thicker than the main part of the ribbon. At the point at which two ribbons crossed they often showed flattened patches surrounded at their edges by narrowed necks of ribbon (figure 1) suggesting that the ribbons' surfaces adhered tightly when brought close together. The surfaces of the ribbons appeared almost completely smooth even at the highest magnification, showing no evidence of a special adhesive coating. These observations suggest that, as in the fine hairs on the surface of the gecko's feet (Autumn *et al.* 2000) or the hackled threads of the cribellate spiders (Opell 1995; Vollrath 1994), van der Waal's forces are responsible for the adhesion of the ribbons to one another and to the prey.

Numerous fractured, or partly fractured, ribbons were seen in SEM preparations. The fracture appeared brittle and always ran perpendicularly across the ribbon with little observable deviation around the nanofibrils (see below) of the ribbon (figure 2). This fracture behaviour is similar to that of synthetic composites containing elastomeric polymers (Chang *et al.* 1992).

The ribbons were remarkably stable in TEM. Their extreme thinness, probably of the order of tens of nanometers, is confirmed by the observation that double-stained preparations show high transparency to electrons, excellent resolution and are apparently constructed from only a single incomplete layer of nanofibrils (figures 3 and 4).

In TEM, the ribbons show an increase in density at their very edges confirming an increase in thickness here (figure 3). This would help to prevent crack initiation at

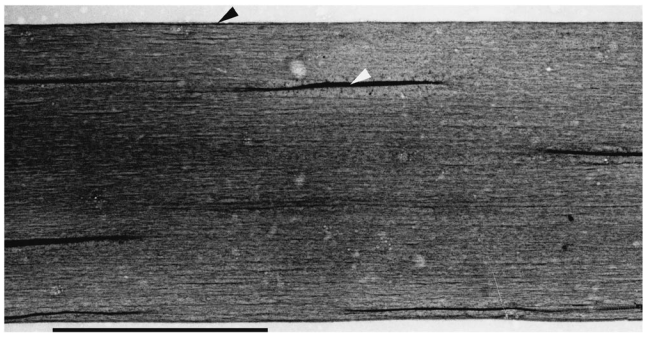

Figure 3. TEM micrograph of a stained silk ribbon. The ribbon is denser at its edge (black arrowhead) and tends to fold longitudinally (white arrowhead). Scale bar, 5 μm.

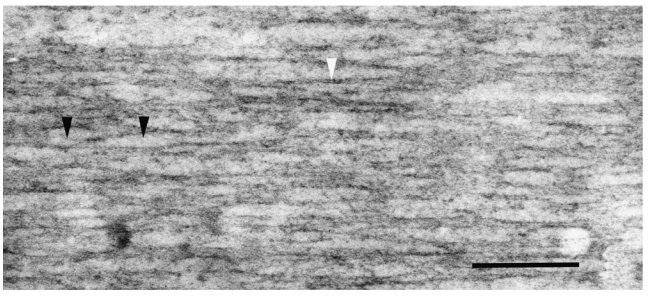

Figure 4. As figure 3 but at higher magnification showing nanofibrils deflected around less dense lens-shaped areas (black arrowheads). The nanofibrils frequently appear double (white arrowhead). Scale bar, 250 nm.

the edges of the ribbon. In TEM, the ribbons contain numerous fine filaments with an apparent diameter of *ca*. 2–4 nm (figure 4). These frequently run in pairs to produce a nanofibril with a diameter of $12 \pm 2$ nm ($n = 10$). The nanofibrils are orientated almost parallel to the long axis of the ribbon forming a markedly anisotropic meshwork with rather large spaces between the nanofibrils. In places, the filaments deflect around convex lens-shaped areas with lower density (figure 4) suggesting that there are at least two components to the ribbon, the nanofibrils and an amorphous less dense component between them. The low packing density of nanofibrils in the ribbons of *Loxosceles* is in marked contrast to the high density seen in fibres dispersed from the dragline silk of the orb web spider *Nephila edulis* (Knight & Vollrath 2001) and may reflect the fact that the latter, unlike the former, is designed for extreme toughness. The marked anisotropy in the arrangement of nanofibils in the ribbons of *Loxosceles* probably accounts for its tendency to form longitudinal folds (figure 3).

### (b) *Gross morphology of MA gland and duct*

Figure 5 summarizes the parts of the MA gland and associated duct in *L. laeta*. Though the glandular portion occupies about two-thirds of the combined length of the gland and duct, it was much shorter in relation to the length of the abdomen compared with the equivalent structure in orb web spiders (Knight & Vollrath 1999*a*). This probably correlates with a much smaller production of silk compared with orb web spiders. Figure 6 shows a pair of somewhat sac-shaped glands running for much of the length of the abdomen and located close to the ventral

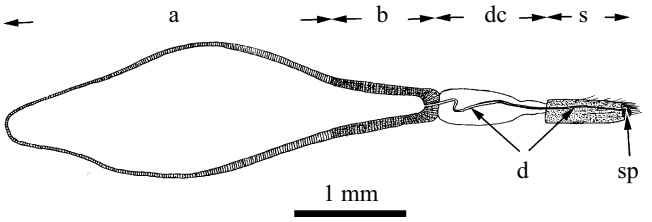


Figure 5. Drawing from micrographs of the MA gland of the adult female *Loxosceles laeta*. Abbreviations: a, zone A; b, zone B; dc, duct cell; s, spinneret; sp, spigot. Scale bar, 1 mm.

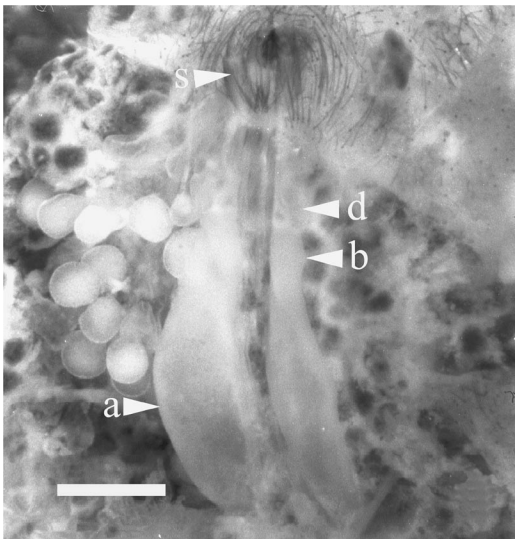


Figure 6. Dissection showing ventral view of the abdominal contents of a female spider fixed in Karnovsky solution. The MA gland and associated duct runs for much of the length of the abdomen and is connected to the anterior spinneret (s). The glandular portion has separate zones A and B (a and b, respectively). The duct region (d) is sharply divided from the glandular portion. Scale bar, 1 mm.

surface. The gland contributes its secretion to a duct that can be followed by dissection to a single large spigot located sub-terminally and medially on the short terminal segment (turret) of the anterior spinneret (figure 7). The position and size of the spigot relative to that of the 9–11 pyriform spigots found apically on the anterior spinneret (figure 12) closely resembles that of the MA gland of araneomorph spiders (Coddington 1989). The MA duct in *Loxosceles* has a small S-bend (figure 8) much less pronounced than that in orb web spiders (Knight & Vollrath 1999*a*) and tapers only slightly as it runs towards the spigot. Thus, the morphology of the gland and duct portions and the position and size of the spigot indicate a close homology to the MA gland of araneomorphs though the proportions of the gland and duct are markedly different from those of orb web spiders.

The duct in *Loxosceles* simply emerges from between the columnar cells at the distal end of the glandular portion (figure 8) without the marked cuticular thickening ('funnel') (Vollrath & Knight 2001) seen in orb web spiders. This gives the junction between gland and duct an appearance more closely resembling that of the presumed ancestral pyriform-type gland (Glatz 1973; Haupt & Kovoor 1993). The 'valve' of orb web spiders is also

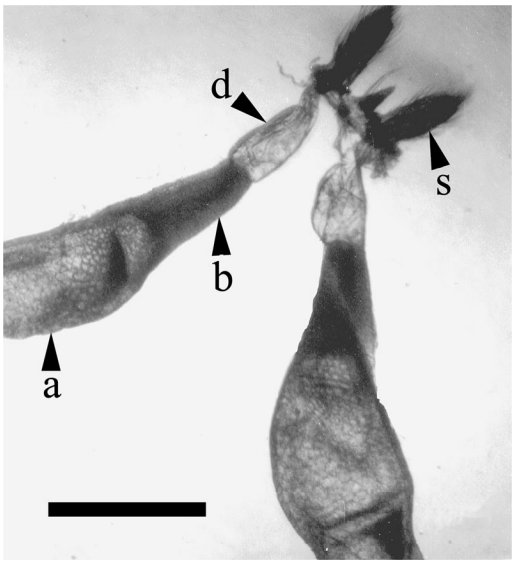


Figure 7. Cleared unstained whole mount of the MA gland (bright field illumination). Labels as for figure 6. The duct region is attached to the anterior spinneret. Scale bar, 1 mm.

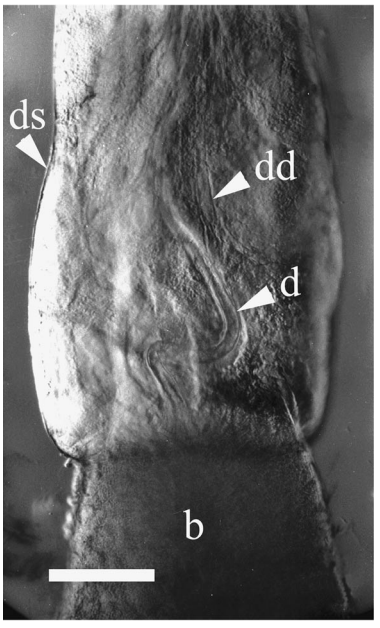


Figure 8. Differential interference micrograph of preparation as in figure 7. The duct (d) is S-shaped and remarkably short in this species. The cuticle lining of the duct appears to be secreted by a cylinder of duct epithelial cells surrounded by a thin sheath (ds). The duct cells are clearly demarcated from the B-zone cells (b). The degenerating duct (dd) is probably derived from the previous instar. Scale bar, 100 μm.

absent in *Loxosceles*. This structure, at the distal end of the duct in orb web spiders, is thought to act as a clamp to help control the spider's descent on the dragline (Wilson 1962). This function is vital to web building in orb web spiders but not in the far less acrobatic and more earth-bound *Loxosceles*.

The flasked-shaped cells found beneath thinnings of duct cuticle just before the valve (Vollrath & Knight 1998, 2001) are absent in *Loxosceles*. This is compatible with the suggestion (J. Kovoor, personal communication) that they

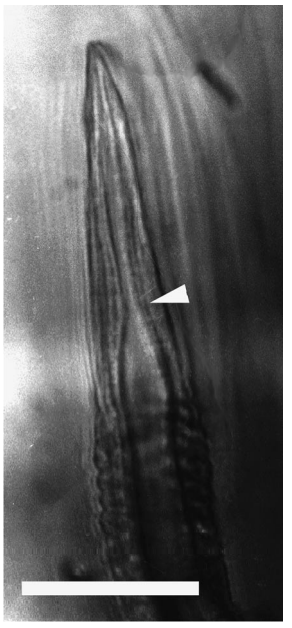

Figure 9. As figure 8 but showing the MA spigot sideways on (compare with). The lumen constricts markedly in the plane of the optical section (arrowhead) to give the narrow but highly elongated exit slit seen in figure 10. Scale bar, 10 μm.

Figure 10. SEM micrograph showing the MA spigot. The outer exit (the top of the image) is a markedly elongated slit. Corrugations at the base of the spigot may prevent kinking when the spigot flexes during spinning while longitudinal ridges on the distal part may stiffen the crucial part of the extrusion die containing the constriction (see figure 5). The flexible lips (arrowhead) lack ridges. Scale bar, 15 μm.

apply pheromones (Schultz & Toft 1993) to the frame and radial threads in orb web spiders.

### (c) *Morphology of the MA spigot*

Figures 9 and 10 show micrographs of the spigot. This structure is *ca.* 45 μm long and is much less gracile than the pyriform, asciform and single minor ampullate or


Figure 11. SEM micrograph showing highly modified comb-like hairs (c) found only on the apex of the posterior lateral spinneret. These may help the spider to position and press together the silk ribbons spun from the MA spigot. Scale bar, 20 μm.

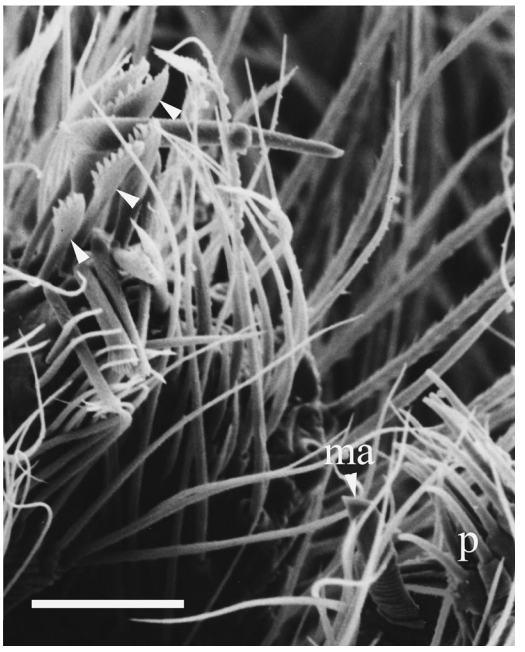


Figure 12. SEM micrograph showing the size and position of the comb-like spines (arrowheads) on the posterior lateral spinneret in relation to the MA spigot (ma) and a group of pyriform spigots (p) mounted on the anterior spinneret. Scale bar, 10 μm.

cylindriform spigot on the posterior median spinnerets in this species. The lumen of the MA duct is practically circular in cross-section where it enters the spigot and it continues without appreciable change in diameter through the annulated basal part (figure 9). Below this it constricts dorsoventrally to about one-third of its diameter. After this constriction, the lumen continues, without a marked change in shape, to discharge at a narrow exit slit measuring *ca*. 10 μm wide and *ca*. 0.275 μm thick (figure 10) though the internal functional opening of the exit is probably much thinner. The outermost ends of the exit slit are appreciably thicker than the rest of the slit and this is thought to form the thicker edges of the ribbon (see above). The widest axis of the slit is orientated transverse to the animal's antero–posterior axis. This probably helps the spider to apply an even pull across the width of the slit as it draws silk from the spigot. The spigot's internal lumen is thought to function in the following way (see figure 20). Liquid dope is transferred to the spigot and reaches the dorsoventral constriction. Here the convergence of the lumen induces elongational flow that helps to orientate the molecules. Thereafter wall shear in the elongated and highly flattened lumen in the last part of the spigot may further orientate the molecules and induce a strain-induced extension and aggregation of the silk protein molecules (Knight *et al.* 2000; Chen *et al.* 2002) to produce a partially plastic solid. Further draw down of the extremely thin silk ribbon in the air gap may account for the observation that the silk thread is narrower and thinner than the opening of the spigot. This final air draw down is likely to contribute to the molecular alignment and further solidification of the ribbon as in orb web MA silk (Vollrath & Knight 2001).

Fixed whole mounts of the duct and spinneret show no evidence of an internal draw down similar to that seen in orb web spiders (Work 1977; Knight & Vollrath 1999*a*; Vollrath & Knight 2001).

The extreme flatness and smoothness of the silk ribbon extruded in this way may enable it to stick efficiently to itself and to prey using van der Waal's forces rather than a water-based adhesive (see above). The latter would tend to dry out in the relatively dry environment in which the spider lives. Alternatively, the large surface area of the ribbon may enable it to carry a high electrostatic charge. This, in turn, may help the silk ribbons to fly apart and deploy effectively in the space used for the spider's retreat. The greatly broadened comb-like hairs found only on the tip of the posterior spigot (figures 11 and 12) may help to press the ribbons together or direct the silk as it emerges from the MA spigot, the pointed teeth of the comb acting as a low-friction surface or possibly an electrostatic brush.

The annular constrictions in the outer surface of the basal part of the spigot (figures 9 and 10) may serve to provide flexibility yet prevent kinking of the lumen when the spigot bends during spinning, while longitudinal ridges in the cuticle of the outer part may stiffen the crucial constricted region of the die (figure 10).

### (d) *Ultrastructure of the MA gland*

The glandular sac, like that of most arachnid silk glands (Glatz 1973; Work 1984; Kovoor 1987) contains two completely distinct transverse zones. Zone A (located furthest from the spigot) is considerably larger than the more distal zone B. Both zones are constructed from tall columnar cells whose height increases distally in the gland. A single incomplete layer of small basal cells is found between the columnar cells and the basement membrane of the gland (figure 19). These cells are closely similar in appearance to the 'regenerative cells' described by Plazaola & Candelas (1991) in the sac of the MA gland

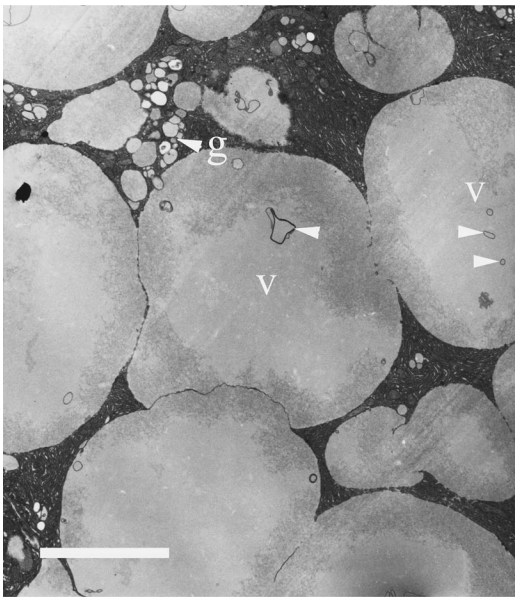


Figure 13. TEM micrograph of an ultrathin section showing part of the cytoplasm of a zone A epithelial cell. The cytoplasm is packed with numerous large secretory vesicles (v) often containing a tangle of fine filaments (see figure 10) and a central clear zone sometimes containing myelin figures (arrowheads). Golgi apparatus (g, arrowhead). Scale bar, 5 μm.

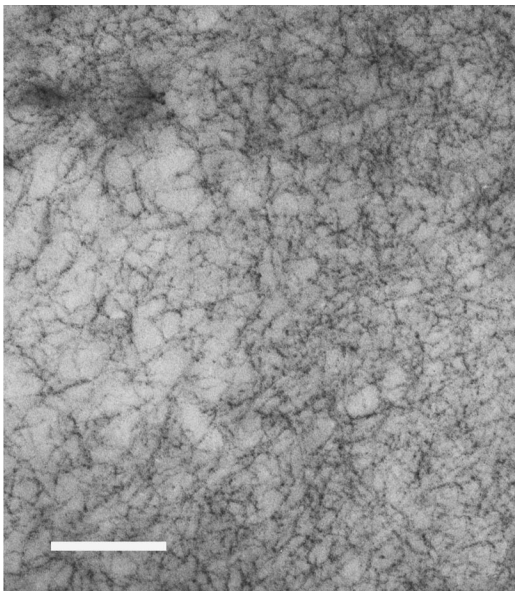

Figure 14. As figure 13 but showing nanofibrils in a zone A secretory vesicle at high magnification. Scale bar, 250 nm.

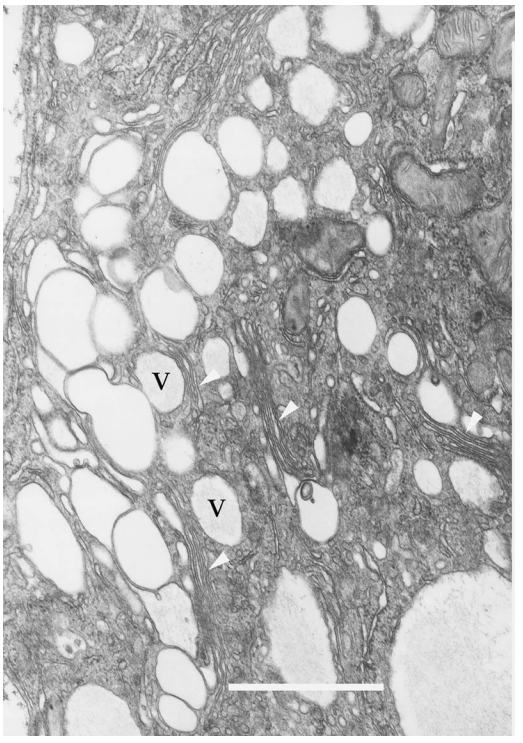


Figure 15. As figure 13 but showing part of the Golgi apparatus of a zone A columnar epithelial cell. Putative developing secretory vesicles (v) contain filaments closely similar to those seen in the mature secretory vesicles. Stacks of flattened Golgi cisternae (arrowheads). Scale bar, 1 μm.

in *Nephila clavipes*. The nuclei of the columnar cells (figure 18) are located basally and are large (up to 50 μm in diameter) approximately five times the diameter of the basal cell nuclei. They contain at least six nucleoli and a very large number of islands of heterochromatin. These features (Luszczek *et al.* 2000) suggest that they may be polyploid, unlike the equivalent nuclei in *Nephila*.

A secretory apparatus is present at the apical pole in both zone A and B columnar cells (figure 17) and is similar to that described by Plazaola & Candelas (1991) but contains a much deeper apical pit.

Zone A columnar epithelial cells are packed with numerous relatively large secretory vesicles (figure 13) with a mean diameter of $9 \pm 2$ μm ($n = 20$) (measured in 5 μm survey sections with a light microscope). In TEM sections, the vesicles frequently contain numerous fine nanofibrils (figure 14) often arranged in a peripheral band surrounding a central clear zone in which myelin figures can often be distinguished (figure 13). The nanofibrils have a diameter of 5–10 nm and are similar to those seen in the secretory vesicles in the proximal tail of zone A in *N. edulis* (D. P. Knight and K. Davies, unpublished data). Regions of sufficiently low fibril density enable the length of the nanofibrils to be estimated at *ca.* 150 nm, in *Loxosceles* zone A secretory vesicles, much shorter than those seen in the final silk (see below). The presence of nanofibrils in the secretory vesicles of zone A suggests that, as in *Nephila* (Vollrath & Knight 2001) this zone elaborates the nanofibrillar component of the finished silk (see above). Zone A secretory vesicles in *Loxosceles*, as in *Nephila* (Vollrath & Knight 2001), appear to be formed in a large Golgi apparatus (figure 15). This can easily be found by searching in a supranuclear region for a concentration of numerous small vesicles (figure 13) some of which have contents similar to those of the mature secretory vesicles. The Golgi apparatus is very similar to that described by Plazoala & Candelas (1991). The cytoplasm in between zone A secretory vesicles contains abundant RERs.

Zone B columnar epithelial cells are also packed with secretory vesicles (figure 17) but these are smaller ($4 \pm 0.5$ μm) and are somewhat more electron dense than those of zone A. They contain dense granular material

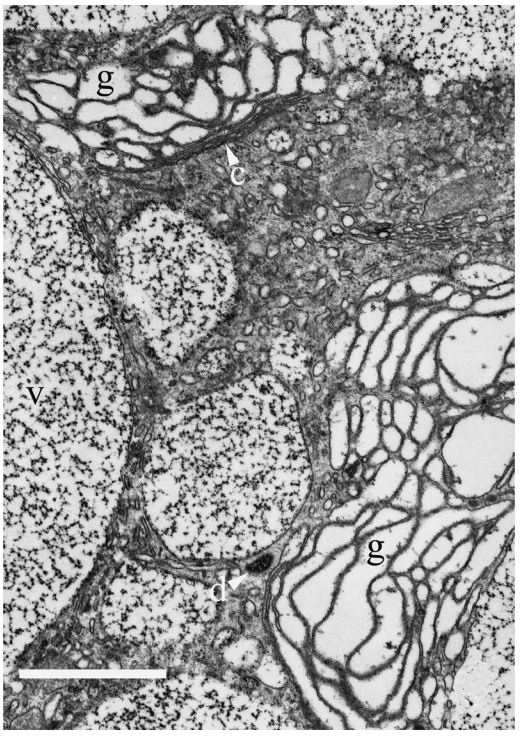


Figure 16. TEM micrograph showing part of the Golgi apparatus (g) of a zone B columnar epithelial cell. The mature secretory vesicles (v) contain dense granules that frequently appear to have clumped into chains. Occasional small vesicles (d, arrowhead) contain what appear to be dense aggregations of these granules. Golgi cisternae (c). Scale bar, 1 μm.

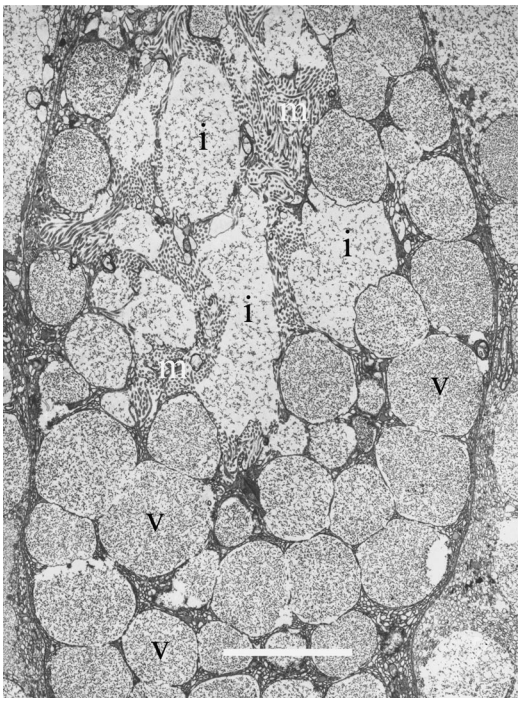


Figure 17. TEM micrograph showing the apical part of a zone B columnar cell. An apical secretory apparatus contains clusters of microvilli (m) surrounding an invagination (i) containing dense granules similar to those found in the numerous mature secretory vesicles (v) packing the cytoplasm. Scale bar, 5 μm.

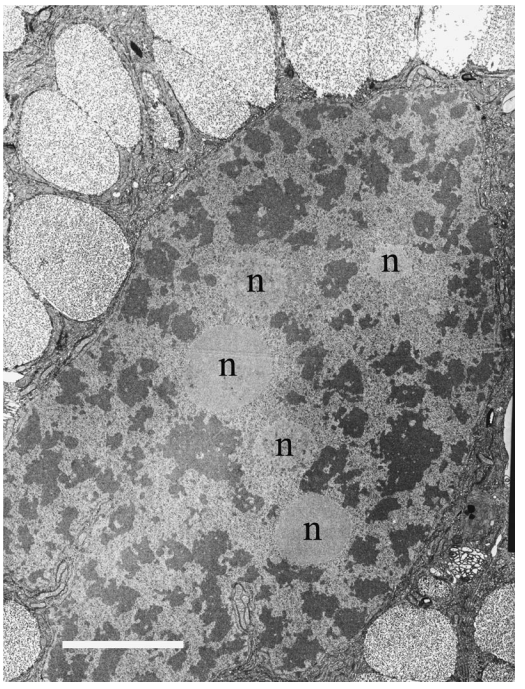


Figure 18. As but showing the basal part of a zone B columnar cell. The large nucleus contains many nucleoli (n) and islands of heterochromatin (see text). Scale bar, 5 μm.

(figure 16) in some places arranged like beads on as string. This material shows no resemblance to that of zone B secretory granules in *Nephila* (Knight & Vollrath 1999*b*). The cytoplasm contains much smooth ER, some RER with a low concentration of ribosomes and only a little RER with abundant ribosomes. This, together with the dense granular appearance of the material in the secretory vesicles could be explained if the cells secreted a phospholipid and a small quantity of protein but we have no histochemical evidence for this. The Golgi apparatus of zone B contains numerous flattened and dilated cisternae giving it an appearance somewhat different to that of zone A (figure 16). Zone B secretion may provide a smooth surface for the ribbon necessary for sticking two ribbons together by van der Waal's forces (see above).

## 4. CONCLUSION

The spider *L. laeta* draws remarkably broad yet thin ribbons of elastomeric silk from its spigot that clearly functions as a sophisticated extrusion die. The large surface area of the ribbon and smoothness of its surface are thought to enable the ribbons to stick together by van der Waal's forces to help the web function as an elastic net. This method of microfabrication may have biomimetic potential.

The observations reported here demonstrate that although the MA gland of *Loxosceles* possess the same basic units (separate transverse zones in the gland, a duct and spigot) seen in other spider silk glands, the detailed construction is remarkably different from that of orb web spiders. One is immediately struck by the relative shortness of the duct and the fact that the opening of the spigot is a highly elongated slit and not a circular opening. We suggest that these design features depend on a fundamental difference between the spinning mechanisms in

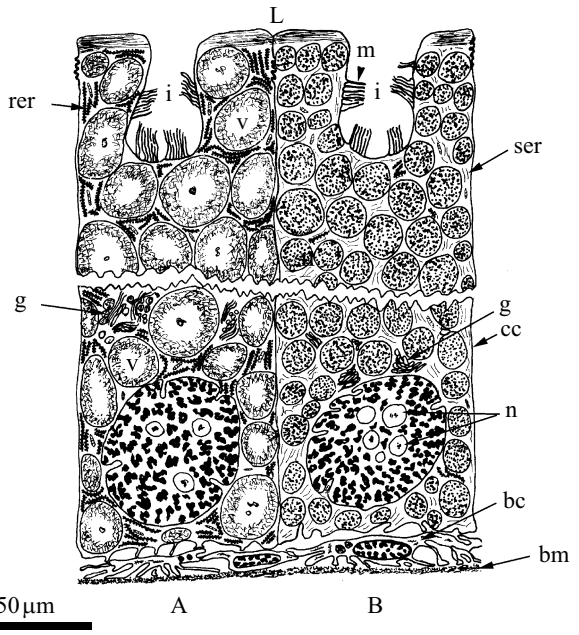


Figure 19. Drawing summarizing the ultrastructure of the junction between zones A and B. Abbreviations: A, zone A; B, zone B; L, lumen; cc, columnar epithelial cell; bc, basal cell; bm, basement membrane; g, Golgi apparatus; V, secretory vesicle; i, invagination; m, microvilli; rer, RER; ser, smooth ER; n, nucleoli. The main differences between zone A and zone B columnar epithelial are: different secretory vesicles and the predominance of RER in zone A cells and smooth in zone B. The drawing shows about half the height of the epithelial cells. Scale bar, 50 μm.

*Loxosceles* and the orb web spiders. The MA gland of orb web spiders, typified by that of *Nephila* spp., produces a cylindrical thread by a mechanism involving an internal draw down starting well inside the distal part of the duct followed by an external draw down in the air after the spigot (Work 1977; Vollrath & Knight 2001). In contrast, *Loxosceles* draws a highly flattened ribbon of silk directly from the spigot without an internal draw down. To do this the dope fed to the spigot must be highly fluid, in contrast to orb web spiders where the dope is thought to be largely solid by the time it reaches the spigot (Knight *et al.* 2000). Thus, *Loxosceles* can manage without the extreme length of the spinning duct required in orb web spiders for forming a solid thread within the spinning duct by secreting $K^+$ and $H^+$ ions and recovering water and $Na^+$ ions (Vollrath *et al.* 1998; Chen *et al.* 2002; Knight & Vollrath 2001; Vollrath & Knight 2001). The long tapering duct in orb web spiders is also thought to produce the extreme elongation of filler particles seen in their dragline silk (Knight & Vollrath 1999*a*) and to spin silk over a huge range of draw rates (Vollrath & Knight 2001). There is no evidence that *Loxosceles* does either of these. The fluidity of the dope in the duct before the spigot in *Loxosceles* probably also correlates with the absence of the clamp-like 'valve' which orb web spiders use like the rock climber's 'descendeur' to control their descent on the dragline (Wilson 1962). Such a clamp would be of no use on the still-fluid silk in *Loxosceles*. The absence of the 'funnel' in *Loxosceles* is intriguing. This structure is a marked thickening of the cuticle between the gland and duct in silk glands with highly elongated ducts (MA, minor ampullate and

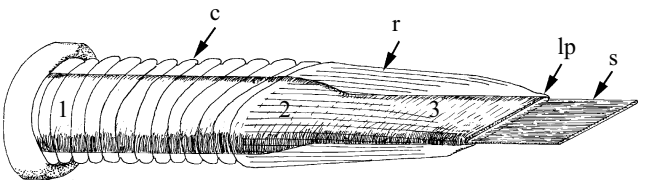


Figure 20. Isometric drawing of the MA spigot (dorsal side up) illustrating the proposed method of action (see text). The spigot is *ca.* 45 μm long and the exit slit *ca.* $10 \times 0.275$ μm. Parallel-sided region of duct with circular cross-section (1), dorsoventral constriction (2), highly flattened part (3), silk ribbon (s), corrugations (c), ridges (r), flexible lips (lp).

cylindriform) in orb web spiders but is absent from glands with a shorter duct (aggregate, pyriform and aciniform). The funnel may serve as a mechanical reinforcement between the elongated and extensible duct and the less mobile glandular portion to prevent premature shear-induced coagulation of the dope when the spider wiggles its abdomen (Vollrath & Knight 2001) or draws silk from the duct. The shortness of the duct and much smaller cross-sectional area of the silk in *Loxosceles* may result in less deformation of the junction between gland and duct, allowing the spider to do without this structure.

Thus, differences between the structure of the MA gland in *Loxosceles* and orb web spiders may reflect differences in the spinning mechanism. This, in turn, probably reflects the different uses to which the two spiders put their MA silks: forming a retreat in *Loxosceles*, and extremely tough threads for major engineering works in orb web spiders. Given the antiquity of the Sicaridae to which *Loxosceles* belongs (Hormiga *et al.* 2000), the simplicity of the MA gland and of its spinning technology compared with that of orb web spiders may represent primitive features (Glatz 1973; Haupt & Kovoor 1993) derived from an ancestral spider and subsequently modified in orb web spinners.

We thank the Danish Science Research Council (SNF), the Science Faculty of Aarhus University, the Carlsberg Foundation, the Danish Academy of Science, the British Biological and Engineering Research Councils (BBSRC, EPSRC), and the European Science Foundation (ESF) for funding; Thomas Vinnman for his generous gift of spiders; and David Kaplan, Beat Meier and John Gosline for helpful discussions; and the Biological Imaging Centre, University of Southampton for their technical assistance.

## REFERENCES

Autumn, K., Liang, Y. A., Hsieh, S. T., Zesch, W., Chan, W. P., Kenny, T. W., Fearing, R. & Full, R. J. 2000 Adhesive force of a single gecko foot-hair. *Nature* **405**, 681–685.

Chang, F. C., Wu, J. S. & Chu, L. H. 1992 Fracture and impact properties of polycarbonate and MBS elastomer-modified polycarbonates. *J. Appl. Polym. Sci.* **44**, 491–504.

Chen, X., Knight, D. P. & Vollrath, F. 2002 Rheological characterization of *Nephila* spidroin solution. *J. Am. Chem. Soc.* (In the press.)

Coddington, J. A. 1989 Spinneret silk spigot morphology: evidence for the monophyly of orb weaving spiders, Cyrtophorinae (Aranaeidae) and the group Theriidae plus Nesticidae. *J. Arachnol.* **17**, 71–95.

Gardner, K. 1998 Talk given at the 2nd Int. Symp. on Silk, June, 1998 University of Virginia in Charlottesville.

Gatesy, J., Hayashi, C., Montriuk, D., Woods, J. & Lewis, R. 2001 Extreme diversity, conservation and convergence of spider silk fibroin sequences. *Science* **291**, 2603–2605.

Glatz, L. 1973 Der spinnapparat der orthognatha (Arachnida, Araneae). *Z. Morph. Tiere* **75**, 1–50.

Gosline, J. M., DeMont, M. E. & Denny, M. W. 1986 The structure and properties of spider silk. *Endeavour* (New Series) **10**, 31–43.

Griswold, C. J., Coddington, J. A., Hormiga, G. & Scharff, N. 1998 Phylogeny of the orb web building spiders (Araneomorphae, Orbiculariae). *Zool. J. Linn. Soc.* **123**, 1–99.

Haupt, J. & Kovoor, J. 1993 Silk-gland system and silk production in mesothelae (araneae). *Ann. Sci. Nat. Zool. Biol. Anim.* **14**, 35–48.

Hormiga, G., Scharff, N. & Coddington, J. A. 2000 The phylogenetic basis of sexual size dimorphism in orb-weaving spiders (Araneae, Orbiculariae). *Syst. Biol.* **49**, 435–462.

Knight, D. P. & Vollrath, F. 1999*a* Liquid crystals and flow elongation in a spider's silk production line. *Proc R. Soc. Lond. B* **266**, 519–523.

Knight, D. & Vollrath, F. 1999*b* Hexagonal columnar liquid crystal in the cells secreting spider silk. *Tiss. Cell* **31**, 617–620.

Knight, D. P. & Vollrath, F. 2001 Changes in element composition in the secretory pathway for dragline silk in a *Nephila* spider. *Naturwissenschaften*. **88**, 179–182.

Knight, D. P., Knight, M. M. & Vollrath, F. 2000 Beta transition and stress-induced phase separation in the spinning of spider dragline silk. *Int. J. Biol. Macromol.* **27**, 205–210.

Kovoor, J. 1987 Comparative structure and histochemistry of silk-producing organs in arachnids. In *Ecophysiology of spiders* (ed. W. Nentwig), pp. 160–186. Berlin: Springer.

Luszczek, D., Swierczynska, J. & Bohdanowicz, J. 2000 Polyploidization of suspensor basal cell in *Triglochin maritimum* L. (Juncaginaceae). *Acta Biol. Crac. Ser. Bot.* **42**, 131–137.

Madsen, B., Shao, Z. & Vollrath, F. 1999 Variability in the mechanical properties of spider silks at three levels: interspecific, intraspecific and intraindividual. *Int. J. Biol. Macromol.* **24**, 301–306.

Opell, B. D. 1995 Do static electric forces contribute to the stickiness of a spider's cribellar prey capture threads? *J. Exp. Zool.* **273**, 186–189.

Plazaola, A. & Candelas, G. C. 1991 Stimulation of fibroin synthesis elicits ultrastructural modifications in spider silk secretory cells. *Tiss. Cell* **23**, 277–284.

Shear, W. A., Palmer, J. M., Coddington, J. A. & Bonamo, P. M. 1989 A Devonian spinneret: early evidence of spiders and silk use. *Science* **246**, 479–481.

Schultz, S. & Toft, S. 1993 Branched long chain alkyl methyl ethers: a new class of lipids from spider silk. *Tetrahedron* **49**, 6805–6820.

Smith, R. L. 1982 *Venomous animals of Arizona*. University of Arizona Press.

Stern, H. & Kullmann, E. 1975 *Leben am seidenen Faden: die rätselvolle Welt der Spinnen*. Munich: Bertelsmann.

Vollrath, F. 1992 Spider webs and silk. *Sci. Am.* **266**, 70–76.

Vollrath, F. 1994 General properties of spider silk. In *Silks polymers: materials science and biotechnology* (ed. D. L. Kaplan, W. W. Adams, C. Viney & B. L. Farmer), pp. 7–28. Washington, DC: ACS Books.

Vollrath, F. & Edmonds, D. 1989 Modulation of normal spider silk by coating with water. *Nature* **340**, 305–307.

Vollrath, F. & Knight, D. P. 1998 Structure and function of the silk production pathway in the spider *Nephila edulis*. *Int. J. Biol. Macromol.* **24**, 243–249.

Vollrath, F. & Knight, D. P. 2001 Liquid crystalline spinning in nature. *Nature* **410**, 541–548.

Vollrath, F., Hu, X. W. & Knight, D. P. 1998 Silk production in a spider involves acid bath treatment. *Proc. R. Soc. Lond.* B **263**, 817–820.

Vollrath, F., Madsen, B. & Shao, Z. 2001 The effect of spinning conditions on silk mechanics. *Proc. R. Soc. Lond.* B. **268**, 2339–2346

Wilson, R. S. 1962 The structure of the dragline control valves in the garden spider. *Q. J. Microsc. Sci.* **103**, 549–555.

Work, R. W. 1977 Mechanisms of major ampullate silk fiber formation by orb web spinning spiders. *Trans. Am. Microsc. Soc.* **96**, 170–198.

Work, R. W. 1984 Duality in major ampullate silk and precursive material from orb-web-building spiders (Araneae). *Trans. Am. Microsc. Soc.* **103**, 113–121.